Journal of Basic and Applied Engineering Research
p-ISSN: 2350-0077; e-ISSN: 2350-0255; Volume 2, Issue 22; October-December, 2015, pp. 1941-1945

http://www.krishisanskriti.org/Publication.html

Effect of Shroud Depth and Advance Pouring Box on Fluid Flow and Inclusion Floatation behaviour in a Slab Caster Steelmaking Tundish

Maqusud Alam[1], Tabish Qamar Hashmi[2] and Md. Irfanul Haque Siddiqui[3*]

[1,2,3]Department of Mechanical Engineering Aligarh Muslim University, Aligarh, India-202002
E-mail: [1]maqusudmce@gmail.com, [2]tabish.hashmi16@gmail.com, [3]irfansiddiqui.me@amu.ac.in

Abstract—*Steelmaking tundish is an important metallurgical reactor, where various processes are carried out in order to make clean steel. In the present work, a three-dimensional numerical investigation has been carried out on two-strand slab caster tundish. The effect of the length of ladle shroud, advance pouring box (APB) and its wall inclination angle have been studied by analyzing the various fluid flow characteristic values of the tundish. Furthermore, tundish with APB has been considered to assess the hydrodynamics of steel flow and inclusion flow behavior inside tundish. The sizes of inclusions have been varied to understand the inclusion floatation phenomenon. The numerical code has first been validated against the experimental observation performed on a reduced scale slab caster tundish made with Perspex sheet and water as working fluid. The results show that ladle shroud length, APB and its wall inclination angle have a significant effect on the fluid flow characteristic of the tundish. Further, the effect of these parameters has also a significant impact on inclusion floatation in the tundish.*

Keywords*: Steelmaking, advance pouring box, shroud, tundish*

1. INTRODUCTION

Continuous casting of steel has become a widely-used process for manufacturing steel products. The requirement of high-performance clean steel and strict control over compositions made the tundish an extensive field of research[1-3]. In the last couple of decades, the tundish is seen as the last metallurgical reactor[4] where alteration can be made according to the cleanliness[5]. The requirement of clean steel has made significantly impact on the amount of production of the stringent quality steel. The increase in throughputs and requirement of larger product dimensions, the production of clean steel has become a challenge for steelmakers[6]. Thus, clean steel and strict composition control are now becoming the primary concern of steelmakers. The researchers across the world have made emphasis on the study of fluid flow phenomenon in tundish in order to optimize the tundish operation and maximize the quality of output[1,7-10]. The fluid flow characteristic of tundish can be altered by changing the various design of tundish furniture i.e., advance pouring box (APB), shroud length, dam, and weir etc[11]. Various researchers have worked on the different design of tundish furniture etc. to optimize the tundish operations and enhance the quality of tundish output. Further, removal of non-metallic inclusions is a challenge for steelmaker due to the availability of very short time period. A modification in melt flow in tundish can change the course of inclusion floatation and further it can maximize the inclusion removal. The modification of melt flow can be done by minimizing the stagnant volume fraction and optimizing the flow conditions in the tundish. The change in tundish design has a significant impact on intermixing phenomenon inside the tundish The fluid flow characteristics are dependent upon certain design parameters of the tundish[12,13]. Very little information is available on the effect of design parameters particularly the design of APB and shroud depth. These parameters affect the fluid flow configuration inside the tundish and hence, their effect on the fluid flow characteristic will be an interesting and useful observation for the steel industries

In present work, physical and numerical investigations have carried out on two strand slab caster tundish. A numerical model has been validate against the experimental results obtained from water modelling studies. The effect of shroud depth into tundish bath and wall inclination angle of APB has been studied by analysing the various fluid flow characteristic of the tundish. Furthermore, inclusion floatation behaviour inside tundish and its removal have been studied by considering different sizes of non-metallic inclusions.

2. PHYSICAL DESCRIPTION

1 shows schematic diagram of experimental setup and dimensions of full-scale tundish as well as advanced pouring box (APB) respectively. A reduced scale model (scale factor of $\lambda = 1/3$) of six strand boat shape billet caster tundish made of the transparent thermoplastic acrylic sheet has been used for water modeling. The dimensional analysis requires similarity of different dimensionless numbers such as Re, Fr, Ri and We etc for reduced scale laboratory setup. The flow behavior inside tundish is largely affected by these dimensionless

numbers. It is impossible to accurately maintain both Reynolds and Froude similarity simultaneously in reduced scale modeling studies using fluid of similar kinematic viscosity. So, it is assumed that flow phenomena in tundish are largely dominated by the inertial and gravitational forces (i.e., Froude number) rather than the viscous forces (Reynolds number)[5]. In this case, geometric similarity has been maintained by keeping the dimensions of the model and industrial tundish in the same ratio and dynamic similarity is achieved by considering the inertial, viscous and gravitational forces. Pure water was used as a fluid medium (at room temperature) as it has equivalent kinematic viscosity to molten steel. The water model has a close resemblance of flow dynamic properties to the industrial size tundish and hence, sufficient accuracy of theiso-thermal study of steel flow in tundish is expected[14]. Table 1 shows the characteristic parameters of reduced scale model and full-scale tundish.

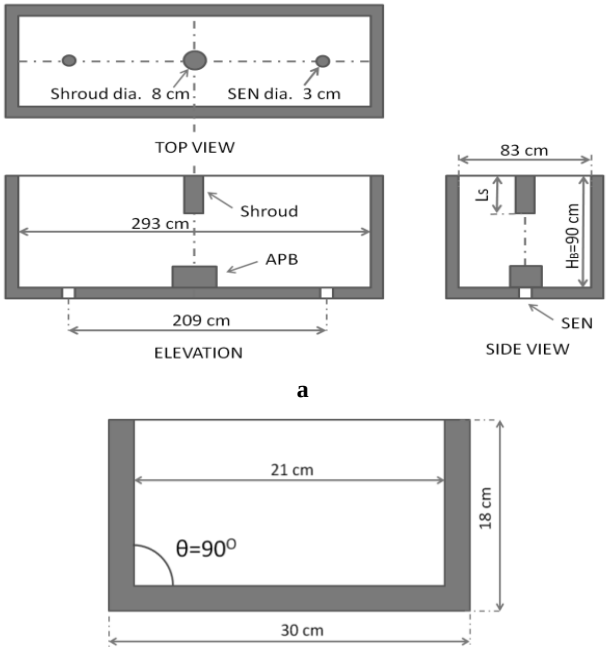

Fig. 1: Diagram and Experimental Setup

Table 1: Characteristic parameters of the model and full-scale slab caster tundish at steady state operating condition.

Parameters	λ= 1/3 Scale model tundish	Full scale tundish
Inflow rate	$0.2\text{x}10^{-3}$ m^3/s	$6.4\text{x}10^{-3}$ m^3/s
Bath height	30 cm	90 cm
Length	97.6 cm	293 cm
APB height	6 cm	18 cm
Volume	0.0495 m^3	3.168 m^3
Density	1000 kg/m^3	7020 kg/m^3
Viscosity	0.001 Pa.s	0.0067 Pa.s

3. MATHEMATICAL MODEL

Governing equations

Continuity:

$$\frac{\partial u_i}{\partial x_i} = 0 \quad (1)$$

Momentum:

$$\frac{\partial}{\partial x_i}\rho u_i u_j = \frac{\partial P}{\partial x_i} + \frac{\partial}{\partial x_i}\left(\mu_{eff}\left(\frac{\partial u_i}{\partial x_j} + \frac{\partial u_j}{\partial x_i}\right)\right) \quad (2)$$

Where,

$$\mu_{eff} = \mu_0 + \mu_t = \mu_0 + \rho C_\mu \frac{k^2}{\varepsilon}$$

Energy equation:

$$\frac{\partial}{\partial x_i}\left(\rho u_i h\right) = \frac{\partial}{\partial x_i}\left(k_{eff}\right)\frac{\partial T}{\partial x_i} \quad (3)$$

Concentration,

$$\frac{\partial(\rho C)}{\partial t} + \frac{\partial\left(\rho u_i C\right)}{\partial x_i} = \frac{\partial}{\partial x_i}\left(\frac{\mu_{eff}}{\sigma_c}\frac{\partial C}{\partial x_i}\right) \quad (4)$$

Theoretical mean residence time,

$$\tau = \frac{\text{Volume of the tundish}}{\text{Volumetric flow rate}} \quad (5)$$

Actual Residence Time,

$$t_r = \frac{\sum C_{avi} t_i}{\sum C_{avi}} \quad (7)$$

In equation (8), the integration is carried over a time span 2τ with an equal interval of time step

$$\text{Fraction of dead volume of the tundish} = 1 - \frac{t_r}{\tau} \quad (8)$$

Break through time, t_p = First appearance of tracer at the exits (9)

$$\text{Fraction of plug volume} = \frac{V_p}{V} = \frac{t_p}{\tau} \quad (10)$$

$$\text{Fraction of mixed volume} = \frac{V_m}{V} = 1 - \left(\frac{V_p}{V} + \frac{V_d}{V}\right) \quad (11)$$

3.2 Turbulence Models

The standard k-ε[3] turbulence model in which the solution of two separate transport equations, allows the turbulent velocity and length scales to be independently determined. Governing equations for turbulent kinetic energy (K) and that for rate of dissipation of turbulent kinetic energy(**ε**) are as follows:

$$\frac{\partial}{\partial t}(\rho K) + \mathbf{div}(\rho K U) = \mathbf{div}\left[\left(\frac{\mu_t}{\sigma_k}\right)\mathbf{grad}\, K\right] + 2\mu_t S_{ij}.S_{ij} - \rho\varepsilon \quad (12)$$

$$\frac{\partial}{\partial t}(\rho\varepsilon) + \mathbf{div}(\rho\varepsilon U) = \mathbf{div}\left[\left(\frac{\mu_t}{\sigma_\varepsilon}\right)\mathbf{grad}\varepsilon\right] + C_{1\varepsilon}\frac{\varepsilon}{K}2\mu_t S_{ij}.S_{ij} - C_{2\varepsilon}\rho\frac{\varepsilon^2}{K} \quad (13)$$

The turbulent (or eddy) viscosity, μ_t, is computed by combining k and ε as

$$\mu_t = \rho C_\mu \frac{K^2}{\varepsilon}$$

where, C_μ is a dimensionless constant. According to the recommendations of Launder et al. for turbulent flows, following values have been adapted for constants[4]

$C_{1\varepsilon}$=1.44, $C_{2\varepsilon}$= 1.92, C_μ=0.09, σ_k=1 and σ_ε=1.30

Reynolds stresses are computed by the following Boussinesq relationship[5]

$$-\rho\overline{u_i'}\overline{u_j'} = \mu_t\left(\frac{\partial U_i}{\partial x_j} + \frac{\partial U_j}{\partial x_i}\right) - \frac{2}{3}\rho k\delta_{ij} = 2\mu_t S_{ij} - \frac{2}{3}\rho k\delta_{ij} \quad (14)$$

3.3 Numerical Details

A three dimensional unstructured tetrahedral mesh was used for numerical simulations. A control volume based technique has been used to convert the governing equations to algebraic equations. Second-order upwind discretization scheme was used to discretize the transport equations. The SIMPLE algorithm was used for pressure-velocity coupling and body force (due to gravity) has been considered. The species equation was solved in the complete flow domain Computation was carried out for half of the tundish because of prevalence of symmetry at the centre plane. Fluid flow in tundish was considered predominantly turbulent, hence, the standard k-ε turbulence model was considered. The species equation was solved in the complete flow domain. The CFD software ANSYS Fluent 13.0 was used for solving the set of equations and generating the results. The side walls and bottom were set to a no slip condition with zero velocity and the turbulent quantity has been set from the logarithmic law of the wall of k-ε models. Turbulence intensity at the inlet was specified at 2 % and at the outlets, atmospheric pressure was assumed to be present. At inlet nozzle, the mean vertical velocity was assumed to be uniform through its cross section and other two perpendicular velocities are assumed to be zero. All velocities were set to zero at any wall. The upper top surface was assumed as a free surface. The top surface was considered as a shear-stress free plane. The predicted flow field information was then used as input for the transport equation for inclusions, which was then solved, taking into account the buoyancy, turbulent dispersion, and the effects of particle size and density. Inclusion trajectories were calculated using a Lagrangian particle tracking method. Statistics were gathered to quantify the fates of 1000 inclusion trajectories for each particle size. The percentage inclusion removal from outlet has been calculated. The inclusion trajectory removal cases inclusions touching the side wall were assumed to reflect. Inclusions that were reaching the top surface were assumed to be trapped and at the outlet they were assumed to be escaped

A well-designed tundish should be able to promote the flotation of inclusion particles. In a quiescent melt, for inclusion particles small enough to obey Stokes' law, the terminal rising velocity of the inclusion particles, V_s may be given by Stokes' relation.

$$V_s = \frac{g(\rho - \rho_p)d^2}{18\mu} \quad (15)$$

The mean local inclusion velocity components, μ_p needed to obtain the particle path, are obtained from the following force balance, which includes drag and buoyancy forces relative to the steel

$$\frac{du_p}{dt} = F_D\left(u - u_p\right) + \frac{g_x\left(\rho_p - \rho\right)}{\rho_p} + F_x \quad (16)$$

4. VALIDATION

Before proceeding with the computation of two strand slab caster tundish, the numerical code has been validated against the experimental result of a water model of two strand tundish for the RTD curve validation in Fig. 2. The experimental result and the computed result nearly match with each other. Thus it is evidently confirmed that the FLUENT based model is able to simulate the observed flow phenomena fairly realistic, as the extent of mismatch between the two curves are not very high.

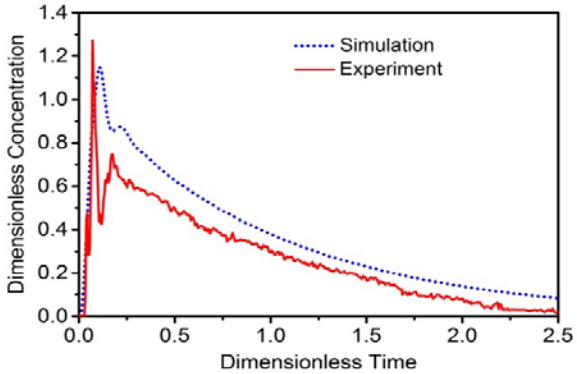

Fig. 2: Comparison between experimental and computed RTD curves

5. RESULTS AND DISCUSSIONS

The numerical investigations have been carried out on various design parameters of two strand slab caster tundish. The effect of RTD parameters have been calculated and are summarized in table 1. The depth of shroud is an important parameter that affects the melt flow profile. It can be seen from Table 1 that the value of t_{min} has increased when the shroud depth was increased. It is observed that an increase in shroud depth has also significant impact over the reduction of dead volume fraction inside tundish.

Table 2: RTD parameters and the associated volume fractions in a two strand bare tundish system

Case	t_{min}	t_{peak}	t_{mean}	θ_{min}	θ_{peak}	θ_{mean}	V_p	V_m	V_d	V_m/V_d	Q_a/Q
Shroud 10%	4	26	293	0.011	0.071	0.801	0.041	0.698	0.261	2.67	0.923
Shroud 15%	4	26	293	0.011	0.071	0.801	0.041	0.698	0.261	2.67	0.923
Shroud 25%	5	27	294	0.014	0.074	0.804	0.044	0.696	0.260	2.67	0.920
Shroud 40%	6	31	298	0.016	0.085	0.817	0.051	0.704	0.246	2.86	0.924
APB 90	10	37	293	0.027	0.101	0.806	0.065	0.683	0.253	2.69	0.927
APB 100	25	57	306	0.069	0.157	0.841	0.113	0.664	0.223	2.97	0.923
APB 110	20	50	305	0.055	0.138	0.841	0.096	0.701	0.202	3.47	0.949
APB 120	17	44	299	0.047	0.121	0.824	0.084	0.749	0.167	4.48	1.01
APB 130	13	41	302	0.036	0.113	0.832	0.075	0.693	0.232	2.98	0.922
APB 140	21	59	303	0.058	0.163	0.836	0.110	0.673	0.217	3.10	0.936

The minimization of dead volume of melt can enhance the tundish operation efficiency and reduces the chances of melt solidification inside tundish.

Fig. 3 shows the velocity vector profile obtained at the inlet plane (ZY) of tundish at different depth of shroud. It is noted here that shroud depth has significantly change the course of melt flow in tundish. The small recirculation of melt can be seen when shroud depth is low

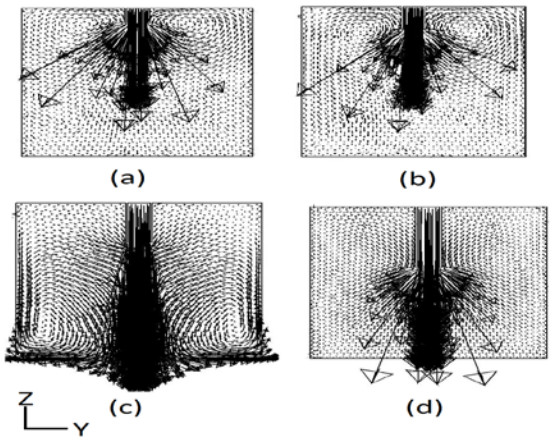

Fig. 3. Shroud depth (a) 10% (b) 15% (c) 25% and (d) 40%.

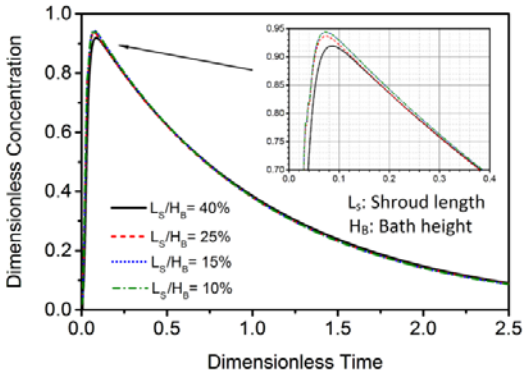

Fig. 4: RTD curves obtained on different design of tundish shroud depth

Fig. 4 shows the C-curve obtained on different design of steelmaking tundish. It is seen here that the peak concentration value of F-curve varies according to shroud depth.

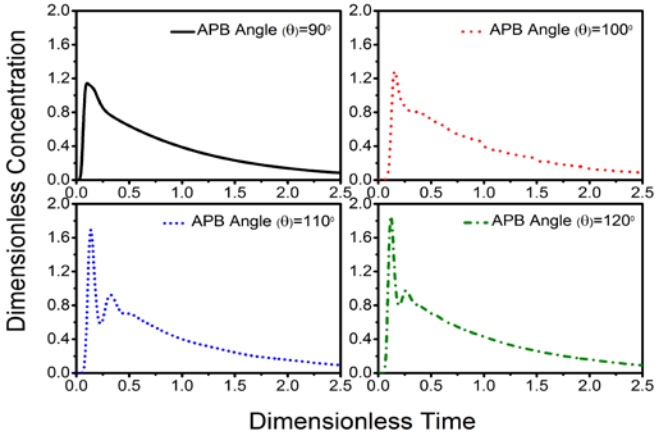

Fig. 5: RTD curves obtained on different design of APB wall inclination angle.

Fig. 5 shows the RTD curve obtained on various wall inclination angle of APB. It is seen that a lower wall inclination angle have more diffusion of incoming melt in tundish. However, an increase in angle has decreased diffusion and mixing tundish.

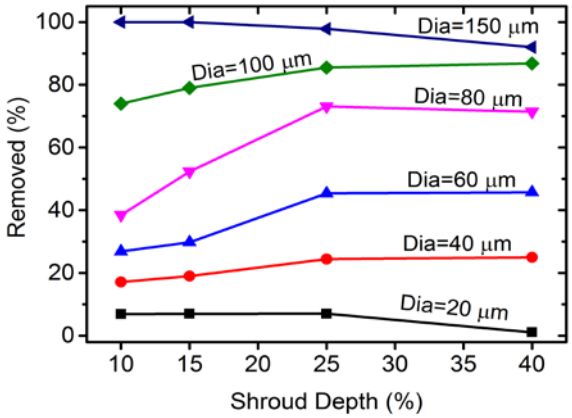

Fig. 6: Percentage removal of inclusion particles in a two strand bare tundish at different shroud length.

In addition to this, inclusion removal and floatation study has been carried out on two parameters of tundish design viz. on shroud depth and wall inclination angle. In this study, various diameters of inclusion has been taken to study the effect of inclusion sizes on floatation phenomenon. Fig. 6 shows the relationship between shroud depth and removal percentage of inclusions. It is seen that maximum percentage of inclusion particles are trapped at shroud depth of 25%.

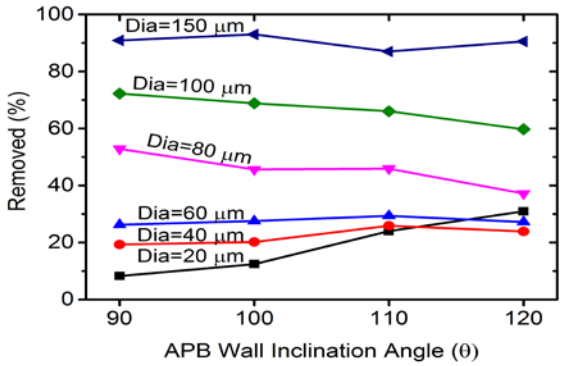

Fig. 7: Percentage removal of inclusion particles in a two strand tundish at different APB wall inclination angle.

However, an opposite phenomenon has been seen when inclusion size is larger i.e., 150μm. It can be also noted that the larger shroud depth i.e., (40%) has no significant impact on inclusion removal from steelmaking tundish. Hence, a lower shroud depth can cause more mixing of inclusion particles in steel products. Furthermore, APB wall inclination angle has also greater impact on inclusion removal. Fig. 7 shows the relationship between APB wall inclination angle and inclusion removal percentage. It is seen that an increase in APB wall inclination angle increases the inclusion removal percentage. However, there is very little impact over the removal of large inclusion diameter

6. CONCLUSION

Physical and numerical investigation has been carried out on two strand slab caster tundish. The numerical code has been validated against the experimental result obtained from reduced scale slab caster tundish. In present study, the effect of shroud depth and wall inclination angle of APB has been studied. The effect of aforesaid parameters have been studied on the basis of characteristic RTD parameters and on removal of inclusion particles from tundish. The sizes of inclusions have been varied to understand the inclusion floatation phenomenon. It is observed that shroud depth and APB wall inclination angle have significant impact on characteristic RTD parameters. The peak value of dimensionless time, mixed and dead volume is greatly affected by the change in each design parameters. Further, the effect of these parameters has also a significant impact on inclusion floatation in the tundish.

REFERENCES

[1] M. I. H. Siddiqui and P. K. Jha, ISIJ Int. **54**, 2578 (2014).

[2] P. K. Jha, R. Ranjan, S. S. Mondal, and S. K. Dash, Int. J. Numer. Methods Heat Fluid Flow **13**, 964 (2003).

[3] S. Joo, J. W. Han, and R. I. L. Guthrie, Metall. Trans. B **24B**, 755 (1993).

[4] A. McLean, in *Proc. Steelmak. Conf. ISS, Warrendale, PA*, (1988), p. 3.

[5] D. Mazumdar, Trans. Indian Inst. Met. **66**, 597 (2013).

[6] D. Mazumdar, O. P. Singh, J. Dutta, S. Ghosh, D. Satish, and S. Chakraborty, Trans. Indian Inst. Met. **64**, 593 (2011).

[7] M. I. H. Siddiqui and P. K. Jha, Steel Res. Int. **85**, 1 (2014).

[8] M. I. H. Siddiqui and P. K. Jha, in *Proc. 22th Natl. 11th Int. ISHMT-ASME Heat Mass Transf. Conf.* (2013).

[9] W. Ahmad and M. I. H. Siddiqui, in *Process. Fabr. Adv. Mater. XXIII* (2014), pp. 994–1009.

[10] M. I. H. Siddiqui and P. K. Jha, in *Int. Conf. Smart Technol. Mech. Eng.* (2013), pp. 122–130.

[11] S. Kant, P. K. Jha, and P. Kumar, Indian Foundary J. **56**, 39 (2010).

[12] C. Chen, G. G. Cheng, H. B. Sun, X. C. Wang, and J. Q. Zhang, Adv. Mater. Res. **476-478**, 293 (2012).

[13] D. Chen, X. Xie, M. Long, M. Zhang, L. Zhang, and Q. Liao, Metall. Mater. Trans. B **45**, 392 (2013).

[14] D. Mazumdar and J. W. Evans, *Modeling of Steelmaking Processes* (CRC Press, 2009).

[15] B. E. Launder and D. B. Spaulding, *Mathematical Models of Turbulence* (Academic Press, 1972).

[16] B. E. Launder, A. Morse, W. Rodi, and D. B. Spalding, in *NASA Conf. Free Shear Flows, Langley* (1972).

[17] J. O. Hinze, *Turbulence* (McGraw-Hill Publishing Co., New York, 1975).